Geophysical Research Letters

RESEARCH LETTER
10.1029/2025GL115280

First Observation of Quenched Davemaoite to Ambient Conditions: Its Electron Diffraction Pattern

Nobuyoshi Miyajima[1], **Lin Wang**[1,2], **and Tomoo Katsura**[1]

[1]Bayerisches Geoinstitut, University of Bayreuth, Bayreuth, Germany, [2]Now at State Key Laboratory of Critical Mineral Research and Exploration, Institute of Geochemistry, Chinese Academy of Science, Guiyang, China

Key Points:

- Submicrometric-sized crystalline Dvm domains exist within an amorphized domain back-transformed from the precursor of a crystalline Dvm grain
- From a selected area electron diffraction pattern of the Dvm domain, Dvm belongs to a cubic symmetry of the space group (S.G. 221) of $Pm\bar{3}m$
- The lattice parameter of $\boldsymbol{a}$ (cubic) = 0.3561(4) nm and the volume $V_0 = 45.16(10)$ Å^3 at 0 GPa (The molar volume, 27.19 cm^3/mol)

Supporting Information:

Supporting Information may be found in the online version of this article.

Correspondence to:

N. Miyajima,
Nobuyoshi.Miyajima@uni-bayreuth.de

Citation:

Miyajima, N., Wang, L., & Katsura, T. (2025). First observation of quenched davemaoite to ambient conditions: Its electron diffraction pattern. *Geophysical Research Letters*, *52*, e2025GL115280. https://doi.org/10.1029/2025GL115280

Received 19 FEB 2025
Accepted 17 JUN 2025

Author Contributions:

Conceptualization: Nobuyoshi Miyajima
Funding acquisition: Nobuyoshi Miyajima, Tomoo Katsura
Investigation: Nobuyoshi Miyajima, Lin Wang
Methodology: Nobuyoshi Miyajima, Lin Wang
Supervision: Nobuyoshi Miyajima, Tomoo Katsura
Writing – original draft: Nobuyoshi Miyajima
Writing – review & editing: Lin Wang, Tomoo Katsura

Abstract Calcium-rich silicate perovskite (davemaoite) has been for the first time investigated at ambient pressure by electron diffraction in transmission electron microscopy. The obtained diffraction pattern in comparison to that of the coexisting Mg-rich silicate perovskite (bridgmanite) has revealed the cubic symmetry, $Pm\bar{3}m$, the lattice parameter $\boldsymbol{a} = 0.3561(4)$ nm and the volume $V_0 = 45.16(10)$ Å^3 (27.19 cm^3/mol), which is still larger molar volume than that of the coexisting bridgmanite (25.49 cm^3/mol). With large volume difference davemaoite and bridgmanite coexist at equilibrium under the conditions at 40 GPa and 2,000°C. The nanometer-sized crystalline davemaoite (4.27 g/cm^3) is mantled by the amorphous $CaSiO_3$ (2.82 g/cm^3). This core-mantle structure prevents amorphization of the unstable high-pressure mineral at the core due to a static pressure, 1.2 (10) GPa generated by volume expansion on the transition at the mantle. This mechanism is the same as that of high-pressure minerals preserved in shocked meteorites.

Plain Language Summary Calcium-rich silicate perovskite, davemaoite is often completely amorphized at ambient pressure, because the perovskite structure containing large element is unstable at 1 bar. However, we obtained for the first time an electron diffraction pattern of davemaoite in a transmission electron microscope. To understand why the unstable crystalline davemaoite lasted so long in the microscope, we investigate the textures with surrounding minerals using the electron-beam imaging and analyze the ambient volume from the diffraction patterns to understand the survival mechanisms. We find that the preservation of the crystalline state is most likely due to a static pressure generated by volume expansion of the surrounding amorphous glass transformed from the precursor denser crystalline state. The mechanism had not been demonstrated experimentally in a sub-micrometer microscopy before, even in the recovery of high-pressure minerals in shocked meteorites. Understanding this mechanism is important because the other high-pressure minerals at a small domain might survive at much lower pressure than the stability field at high pressure even though they are usually unquenchable. Further high-pressure minerals under a static stress can be discovered at ambient conditions by fine electron microscopy.

1. Introduction

The precise volumes of high-pressure minerals at ambient pressure (V_0) are very important for quantitative discussions in the equation of states (EoS) of minerals, for example, a fitting to a second-order Birch–Murnaghan EoS for V_0 (Thomson et al., 2019). The recovered high-pressure samples can be used for further physical and chemical measurements, even though they are metastable at ambient conditions. Calcium-rich silicate perovskite, davemaoite (Dvm) is a stable mineral under the extreme high-pressure conditions corresponding to the bottom of the Earth's lower mantle (L. Wang et al., 2025), but usually unquenchable to ambient conditions. In the literature, a small amount of Dvm has been identified by X-ray diffraction and nuclear magnetic resonance spectroscopy in samples recovered from 15 GPa and 1,500°C (Kanzaki et al., 1991). In their recovered Dvm, the existence of the reflections could not be indexed with the cubic unit cell, indicating that the symmetry of the Dvm is lower than cubic (Kudoh & Kanzaki, 1994). In the same context, orthorhombic $CaSiO_3$ perovskite (Nestola et al., 2018) was reported as an inclusion in a natural diamond. Recently, Ishii et al. (2022) has reported weak X-ray diffraction peaks of Dm at ambient conditions in a normal mid-ocean ridge basalt composition and speculate that the synthesis at higher pressure from 27 to 52 GPa at 2,000 K enhances recoverability of Dvm. To clarify the symmetry and the mechanisms of the presence of the crystalline Dvm at ambient conditions, we investigate a recoverable Dvm domain and its symmetry at the sub-micrometer scale by transmission electron microscopy (TEM). We present for the first time a selected area electron diffraction (SAED) pattern of Dvm in comparison to that of the coexisting with Al, Fe-bearing bridgmanite (Bdm).

2. Materials and Methods

2.1. Observed High-Pressure Minerals

A high-pressure assemblage of Dvm and Bdm phases (Run Iris-1272) was synthesized at 40 GPa and 2,000°C for 24 hr, by using a 15-MN ultrahigh-pressure multi-anvil press (IRIS-15) equipped with the Osugi-type guide-block system at Bayerisches Geoinstitut (BGI), University of Bayreuth. The anvils at the second stage in the compression system were 8 tapered tungsten carbide anvils. Three anvil faces around a truncation of the second-stage anvils were tapered by 1°. The detail procedure of the high-pressure experiment was described in Ishii et al. (2019) and L. Wang et al. (2025).

2.2. Transmission Electron Microscopy (TEM)

The recovered sample from the high-pressure experiment was characterized by using a scanning transmission electron microscope (FEI Titan G2 80-200 S/TEM) at BGI. A thin TEM foil of the recovered sample was prepared with a dual beam focused ion milling machine. Conventional TEM observation and SAED were carried out under a low electron dose (e.g., the probe current less than 700 and 80 pA in the TEM mode and scanning mode, respectively) at 200 kV acceleration voltage. An electron transparent thin lamella was micro-sampled by using a FIB (FEI Scios FIB-Dual beam SEM). The detail procedure of the FIB work was described in Miyajima et al. (2019). In comparison and for the calibration of the camera length on the TEM-electron diffraction, the coexisting Bdm was also investigated by the same TEM system. The accuracy and precision of the lattice parameter of Dvm depend on the following procedure (The supplemental materials including Figures S1–S3 and Table S1 in Supporting Information S1). The camera length of SAED patterns of the Dvm and Bdm was at first calibrated with a Si standard TEM foil and cross-calibrated with the length of the ***c***-axis of the coexisting Bdm. The lattice parameters of the Bdm were refined with X-ray diffraction method (described in Section 2.3). As shown in Figures 1 and 2, the ***c***-axis of the Bdm and the ***a***-axis of Dvm are almost parallel in the recorded CCD images, which minimalize errors in measurements of distances between diffraction spots due to a distortion of the CCD camera. The measurements of the reciprocal distances in SAED patterns were performed with 10 individual distances. The errors are a standard deviation in sampled distances. The cation numbers per formula unit of the coexisting Dvm and Bdm are Ca 0.98(3), Al 0.03(0), Si 0.99(2), Mg 0.005(4) and Mg 0.62(2), Fe 0.37(3), Al 0.34 (2), Si 0.66(2), and Ca: 0.004(2), respectively, based on Oxygen = 3, which were determined by using energy-dispersive X-ray spectroscopy in the TEM. Namely, the davemaoite is nearly pure $CaSiO_3$.

2.3. Micro-Focused X-Ray Diffraction

In comparison to the electron diffraction, the lattice parameters of the coexisting Bdm were determined by using a micro-focused beam X-ray diffraction machine (*Bruker AXS D8 Discover*) equipped with a two-dimensional solid-state detector and a micro-focus source of Co-Kα radiation operated at 40 kV and 500 μA at the BGI. The exposure time was over 1 hr. The obtained diffraction pattern is least square fitted with the structure factor weighted method to refine lattice parameters. The 2 theta values in the X-ray diffraction measurement were externally calibrated with a silicon standard (***a*** = 0.5431 nm). The refined lattice parameters of the coexisting Bdm (Iris-1272) are ***a*** = 0.4809(4), ***b*** = 0.5002(5), and ***c*** = 0.70389(6) nm (Figure S1 in Supporting Information S1).

3. Results and Discussion

3.1. Davemaoite Coexisting With Al, Fe-Bearing Bridgmanite

In bright-field TEM images, submicrometric-sized crystalline Dvm domains exist within an amorphized domain back-transformed from the precursor of a crystalline Dvm grain (Figure 1). Figure 1a displays the coexistence of the Bdm and Dvm grains. The SAED pattern of the Dvm domain (Figure 1b) are consistent with the cubic space group (S.G.) of $Pm\bar{3}m$. The interpretation from the extinction rules of the space group in the electron diffraction pattern is provided in Figures S2–S4 in Supporting Information S1. A refined lattice parameter from the SAED pattern is ***a*** (cubic) = 0.3561(4) nm and the volume V_0 = 45.16(10) $Å^3$ (27.19 cm^3/mol). The indexing on the SAED pattern makes a proof of no extinction rule along the <h00>* direction, because the 100 spot with h = odd and d-spacing = 0.35 nm is visible. The obtained lattice parameter of Dvm (Table S1 in Supporting Information S1) is comparable with the literature data that the lattice parameters extrapolated to 0 GPa by an equation of state were

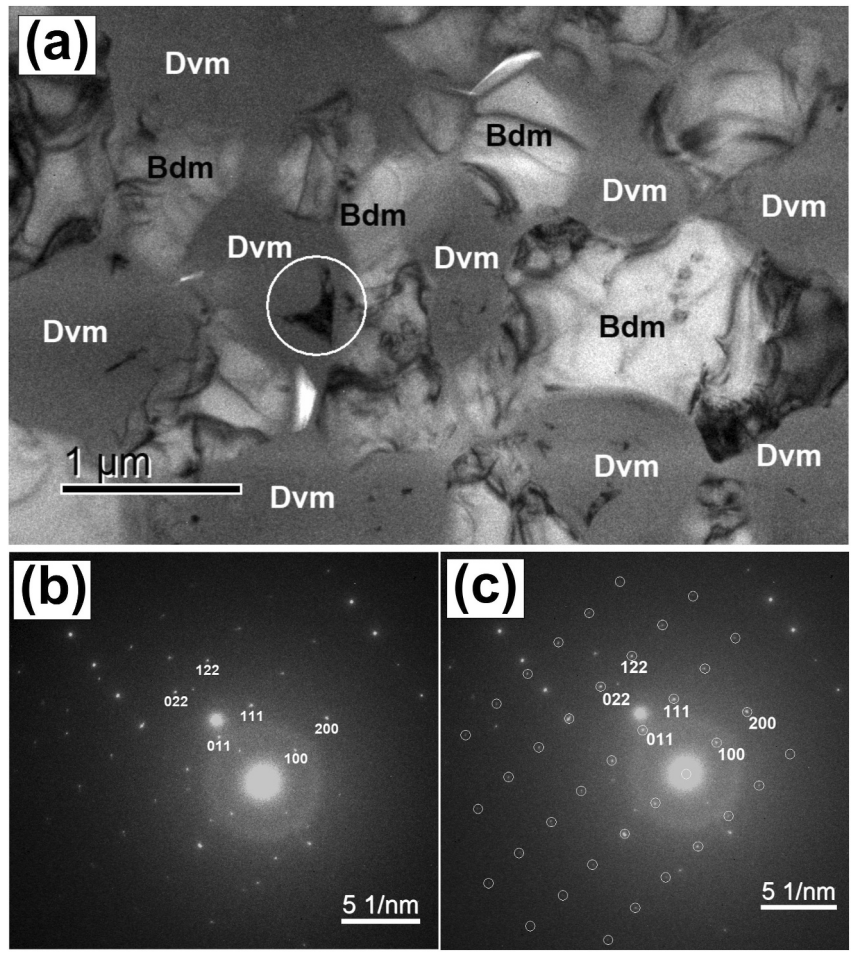

Figure 1. (a) Bright-field transmission electron microscopy image of a quenched davemaoite (Dvm, a black domain indicated by a white circle) in the core and its amorphous domains (gray domains) in the mantle. The surrounding amorphous domains and the coexisting bridgmanite grains (Bdm, white domains) preserve an internal pressure preventing the complete amorphization of Dvm. (b) The corresponding selected area electron diffraction (SAED) pattern from the Dvm domain (indicated by white circle) along the <0$\bar{1}$1> zone axis. The first halo ring corresponds to 0.2939 nm (0.3010 nm by Si correction), while the d-spacing of (100) in davemaoite is 0.3468 nm (0.3561 nm by Si correction). The halo ring corresponds to Si-Si and Ca-Si peaks in an amorphous $CaSiO_3$ (Kondo et al., 2024). The strong diffraction spots along the 11-O'clock direction are from the coexisting Bdm grains at the right side of the Dvm domain. (c) Adding a schematic illustration explaining the indexing of the SAED pattern of a single crystal Dvm on the pattern (b).

estimated as $\boldsymbol{a} = 0.3572$ nm ($V_0 = 45.58(4)$ Å^3, the molar volume is 27.45(2) cm^3/mol in Y. B. Wang et al. (1996)) and 0.358 nm ($V_0 = 45.88$ Å^3 in Tschauner et al. (2021)). The smaller volume than that of Y. B. Wang et al. (1996) might be under a residual pressure (discuss it in the next section). However, the lattice parameter of Dvm, 0.3561 (4) nm in the present study, is larger than 0.351 nm of the coexisting Bdm (S.G., *Pbnm*) (Figures 2 and 3), which was calculated from a half of the length of the ***c***-axis (orthorhombic) = 0.702 nm based on the relation that 1/2 ***c*** (orthorhombic) = ***a*** (cubic) in the orthorhombic perovskite structure. It is likely to indicate that these two perovskite-structured minerals should be at equilibrium under the condition at 40 GPa and 2,000°C, because of different volumes of Bdm and Dvm solid solutions, which are derived from Gibbs free energy in a function of composition, temperature, and pressure, could stabilize their two perovskite-structured phases.

3.2. The Mechanisms to Prevent Complete Amorphization of Davemaoite

The mechanisms to prevent a complete amorphization of Dvm on the decompression to ambient pressure should be explained from the microtextures displaying a core-rim structure where consists of remaining crystalline domain of Dvm at the core part and amorphous domains at the rim (Figure 1 and Figure S5 in Supporting Information S1). The

10.1029/2025GL115280

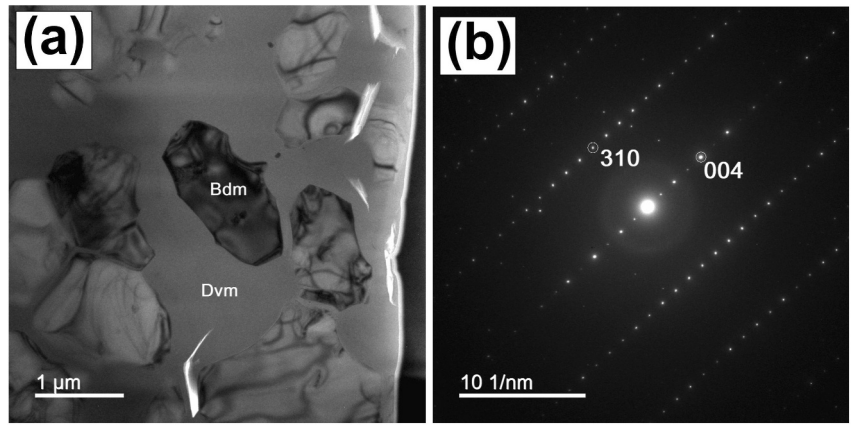

Figure 2. (a) Bright-field transmission electron microscopy image of a coexisting bridgmanite grains (Bdm, black domains). (b) The corresponding selected area electron diffraction pattern (along the [$\bar{1}$30] zone axis) from the Bdm grain, together with a halo ring of the surrounding amorphous Dvm.

density of the amorphous domains with $CaSiO_3$ composition, a glass state is estimated as 2.82 g/cm^3 from a halo-ring with d-spacing = 0.301 nm (Figure 1a), in comparison to the density of $CaSiO_3$ glass, for example, 2.68 g/cm^3 (Yin et al., 1986) and 2.80(5) g/cm^3 (Kondo et al., 2024), while davemaoite is 4.2 g/cm^3 (a = 0.3591(2) nm, Tschauner et al., 2021). The density difference between the glass and crystalline states results in volume expansion upon transition from davemaoite to glass at the current rim. The significant volume expansion due to the amorphization of Dvm induces static stress, that is, an apparent pressure, which prevents the complete amorphization in the core domain at the current ambient pressure. Further, a rigid Bdm framework makes a network over the core-rim structure to keep the pressure in the bulk sample (Figure S5 in Supporting Information S1).

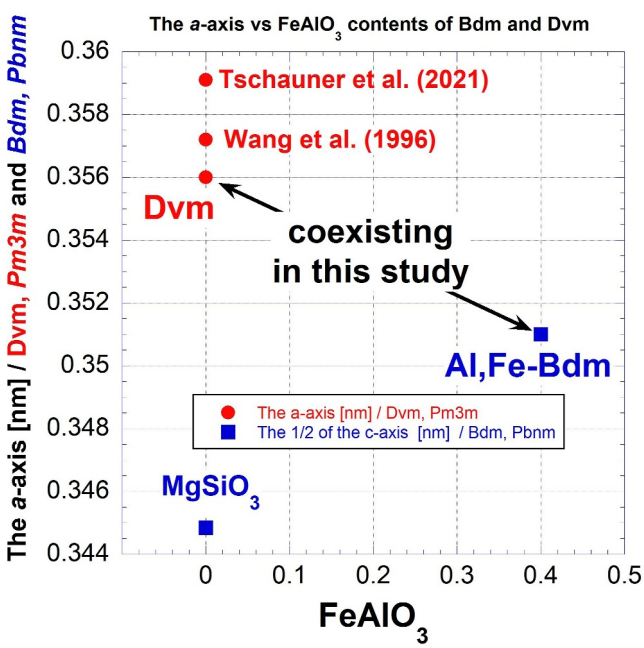

Figure 3. The plot of the a-axis of quenched Dvm (red circles) and a half of the c-axis of the coexisting Bdm (blue squares), in comparison to the literature data. The X-axis of the plot is a function of $FeAlO_3$ component in the Bdm data. Note: The mineral formula of the Dvm in Tschauner et al. (2021) is $(Ca_{0.43(1)}K_{0.20(1)}Na_{0.06}Fe_{0.11(1)}Al_{0.08}Mg_{0.06}Cr_{0.04(2)})(Si_{1.0(2)}Al_{0.00(1)})O_3$. The data of Y. B. Wang et al. (1996) is calculated from reported V_0, 45.58(4) Å^3.

The mechanism is the same as the presence of bridgmanite in shocked meteorites (Nishi et al., 2022), in which a significant volume expansion due to the amorphization prevents the progress of the amorphization of crystalline bridgmanite under residual post-shock temperatures at ambient pressure. Nishi et al. (2022) reported that the partial amorphization of a Bdm aggregate at ~550 K induces a static pressure ~0.5 GPa, estimated from thermal volume variations of a partially amorphized Bdm aggregate at high temperature X-ray measurements. They concluded that the static pressure prevents the progress of the amorphization in a shocked meteorite that fell on Earth. In the same context, based on the density difference between Dvm and its glass, the volume expansion in amorphization of Dvm into a glass state is estimated to ~33% at the maximum if all the crystalline Dvm (4.2 g/cm^3) becomes the amorphous state (2.82 g/cm^3) within a rigid frame of Bdm aggregate. However, a residual pressure remained in the current Dvm-bearing aggregate is estimated to 1.2(10) GPa (Figure S6 in Supporting Information S1), based on volume variations at low pressure from 4.1 to 0.6 GPa (Y. B. Wang et al., 1996). The volume difference between 45.16(10) **Å^3** (evaluated in electron diffraction data in this study) and 45.28 **Å^3** (extrapolated to 0 GPa in the decompression data reported in Y. B. Wang et al. (1996)) originates from the residual pressure in the recovered Dvm-Bdm aggregate. Although the density difference between amorphous glass and Dvm crystal is further large, a partial amorphization to the glass state at the pressure release could support some portion of the internal pressure in the surrounding rigid Bdm frame. In those mechanisms, an amorphous fraction during decompression in the high-pressure experiment can facilitate the residual crystalline domains at the nanometer scale. It is a worthy note that Tomioka and Kimura (2003) reported assemblages of majorite garnet and a $CaSiO_3$-rich phase as breakdown products of diopside in a shocked chondritic meteorite. Based on their TEM

observations (Figure 3 in Tomioka and Kimura (2003)), the $CaSiO_3$-rich phase was interpreted as glass, thought to have formed during the release of shock pressure. This interpretation might warrant closer examination, as part of the phase may in fact represent crystalline Dvm.

4. Conclusions

We presented for the first time an electron diffraction pattern of a crystalline Dvm coexisting with Al, Fe-bearing bridgmanite (Bdm) by using SAED in TEM. The symmetry is a cubic with space group $Pm\bar{3}m$ and the volume $V_0 = 45.16(10)$ Å^3 at ambient conditions. Although the volume of davemaoite at ambient conditions (V_0) could not be determined directly due to possible residual pressure in the sample, the obtained volumes of 45.16(10) Å^3 (electron diffraction data) and 45.28 Å^3 (extrapolated to 0 GPa in the decompression data reported in Y. B. Wang et al. (1996)) in this study can be used as a fixed parameter for precise analysis of an EoS to refine the other unknown parameters such as contents of impurity in a solid solution (e.g., Water, Chen et al., 2020; Shim et al., 2022). The preservation of the crystalline state is most likely due to a static pressure generated by volume expansion of the surrounding amorphous glass transformed from the precursor denser crystalline state, further supporting that the other high-pressure minerals at a small domain might survive at much lower pressure than the stability field at high pressure.

Data Availability Statement

Data set archiving for this research is available at Miyajima (2025).

Acknowledgments
Funded by the open-access publishing fund of the University of Bayreuth. We thank Raphael Njul for polishing recovered samples and Dorothea Wiesner for preparing TEM thin foils by using a FIB. We further thank Tiziana Boffa Ballaran for help with X-ray diffraction. We appreciate the Deutsche Forschungsgemeinschaft (DFG) for funding of the FIB facility (Project number 257745926) and the TEM facility (Project number 189856261). This project has received funding from the European Research Council (ERC) under the European Union's Horizon 2020 research and innovation programme (Proposal 787 527). Open Access funding enabled and organized by Projekt DEAL.

References

Chen, H., Leinenweber, K., Prakapenka, V., Prescher, C., Meng, Y., Bechtel, H., et al. (2020). Possible H_2O storage in the crystal structure of $CaSiO_3$ perovskite. *Physics of the Earth and Planetary Interiors*, *299*, 106412. https://doi.org/10.1016/j.pepi.2019.106412

Ishii, T., Liu, Z., & Katsura, T. (2019). A breakthrough in pressure generation by a Kawai-type multi-anvil apparatus with tungsten Carbide anvils. *Engineering*, *5*(3), 434–440. https://doi.org/10.1016/j.eng.2019.01.013

Ishii, T., Miyajima, N., Criniti, G., Hu, Q. Y., Glazyrin, K., & Katsura, T. (2022). High pressure-temperature phase relations of basaltic crust up to mid-mantle conditions. *Earth and Planetary Science Letters*, *584*, 117472. https://doi.org/10.1016/j.epsl.2022.117472

Kanzaki, M., Stebbins, J. F., & Xue, X. (1991). Characterization of quenched high pressure phases in $CaSiO_3$ system by XRD and ^{29}Si NMR. *Geophysical Research Letters*, *18*(3), 463–466. https://doi.org/10.1029/91GL00463

Kondo, N. M., Kono, Y., Ohira, I., Hrubiak, R., Ohara, K., Nitta, K., & Sekizawa, O. (2024). Different structural behavior of $MgSiO_3$ and $CaSiO_3$ glasses at high pressures. *American Mineralogist*, *109*(6), 1045–1053. https://doi.org/10.2138/am-2023-9060

Kudoh, Y., & Kanzaki, M. (1994). On the symmetry of the $CaSiO_3$ perovskite quenched from 15 GPa and 1500°C. *AIP Conference Proceedings*, *309*(1), 795–797. https://doi.org/10.1063/1.46219

Miyajima, N. (2025). TEM data for the first observation of quenched davemaoite to ambient conditions: Its electron diffraction pattern [Dataset]. *University of Bayreuth*. https://doi.org/10.57880/RDSPACE-UBT-47

Miyajima, N., Mandolini, T., Heidelbach, F., & Bollinger, C. (2019). Combining ECCI and FIB milling techniques to prepare site-specific TEM samples for crystal defect analysis of deformed minerals at high pressure. *Comptes Rendus Geoscience*, *351*(2–3), 295–301. https://doi.org/10.1016/j.crte.2018.09.011

Nestola, F., Korolev, N., Kopylova, M., Rotiroti, N., Pearson, D. G., Pamato, M. G., et al. (2018). $CaSiO_3$ perovskite in diamond indicates the recycling of oceanic crust into the lower mantle. *Nature*, *555*(7695), 237–241. https://doi.org/10.1038/nature25972

Nishi, M., Kaneko, A., Ohgidani, H., Dekura, H., Kakizawa, S., Kawaguchi, S., et al. (2022). Bridgmanite freezing in shocked meteorites due To amorphization-induced stress. *Geophysical Research Letters*, *49*(13), e2022GL098231. https://doi.org/10.1029/2022GL098231

Shim, S.-H., Chizmeshya, A., & Leinenweber, K. (2022). Water in the crystal structure of $CaSiO_3$ perovskite. *American Mineralogist*, *107*(4), 631–641. https://doi.org/10.2138/am-2022-8009

Thomson, A. R., Crichton, W. A., Brodholt, J. P., Wood, I. G., Siersch, N. C., Muir, J. M. R., et al. (2019). Seismic velocities of $CaSiO_3$ perovskite can explain LLSVPs in Earth's lower mantle. *Nature*, *572*(7771), 643–647. https://doi.org/10.1038/s41586-019-1483-x

Tomioka, N., & Kimura, M. (2003). The breakdown of diopside to Ca-rich majorite and glass in a shocked H chondrite. *Earth and Planetary Science Letters*, *208*(3–4), 271–278. https://doi.org/10.1016/s0012-821x(03)00049-9

Tschauner, O., Huang, S. C., Yang, S. Y., Humayun, M., Liu, W. J., Corder, S. N. G., et al. (2021). Discovery of davemaoite, $CaSiO_3$-perovskite, as a mineral from the lower mantle. *Science*, *374*(6569), 891–894. https://doi.org/10.1126/science.abl8568

Wang, L., Miyajima, N., Wang, F., & Katsura, T. (2025). Persistence of davemaoite at lower mantle conditions. *Nature Geoscience*, *18*(4), 365–369. https://doi.org/10.1038/s41561-025-01657-9

Wang, Y. B., Weidner, D. J., & Guyot, F. (1996). Thermal equation of state of $CaSiO_3$ perovskite. *Journal of Geophysical Research*, *101*(B1), 661–672.

Yin, C. D., Okuno, M., Morikawa, H., Marumo, F., & Yamanaka, T. (1986). Structural analysis of $CaSiO_3$ glass by X-ray diffraction and Raman spectroscopy. *Journal of Non-Crystalline Solids*, *80*(1), 167–174. https://doi.org/10.1016/0022-3093(86)90391-1

References From the Supporting Information

Nakatsuka, A., Fukui, H., Kamada, S., Hirao, N., Ohkawa, M., Sugiyama, K., & Yoshino, T. (2021). Incorporation mechanism of Fe and Al into bridgmanite in a subducting mid-ocean ridge basalt and its crystal chemistry. *Scientific Reports*, *11*(1), 22839. https://doi.org/10.1038/s41598-021-00403-6